Analysis of Metal Plate-Stringer-Diaphragm Bridge Decks

Analyse de tabliers métalliques renforcés par entretoises longitudinales et transversales

Berechnung von Brückenfahrbahnen aus Metallplatten mit Längs- und Querverstrebungen

D. L. DEAN
Professor of Civil Engineering, North Carolina
State University, Raleigh, North Carolina U.S.A.

R. R. AVENT
Assistant Professor, Civil Engineering, Georgia
Institute of Technology Atlanta, Georgia U.S.A.

Introduction

The object of this paper is the derivation of formulas for the analysis of deck systems constructed of thin plates reinforced and composite with a set of equally spaced longitudinal stringers which are braced by a set of equally spaced transverse diaphragms (see Fig. 1). The formulas will be applicable for the design of cellular decks-systems with both top and bottom plates — as well as orthotropic decks-systems with a top plate only. Specifically, the formulas are for the exact elastic analysis of those systems that 1) are proportioned and detailed so that all
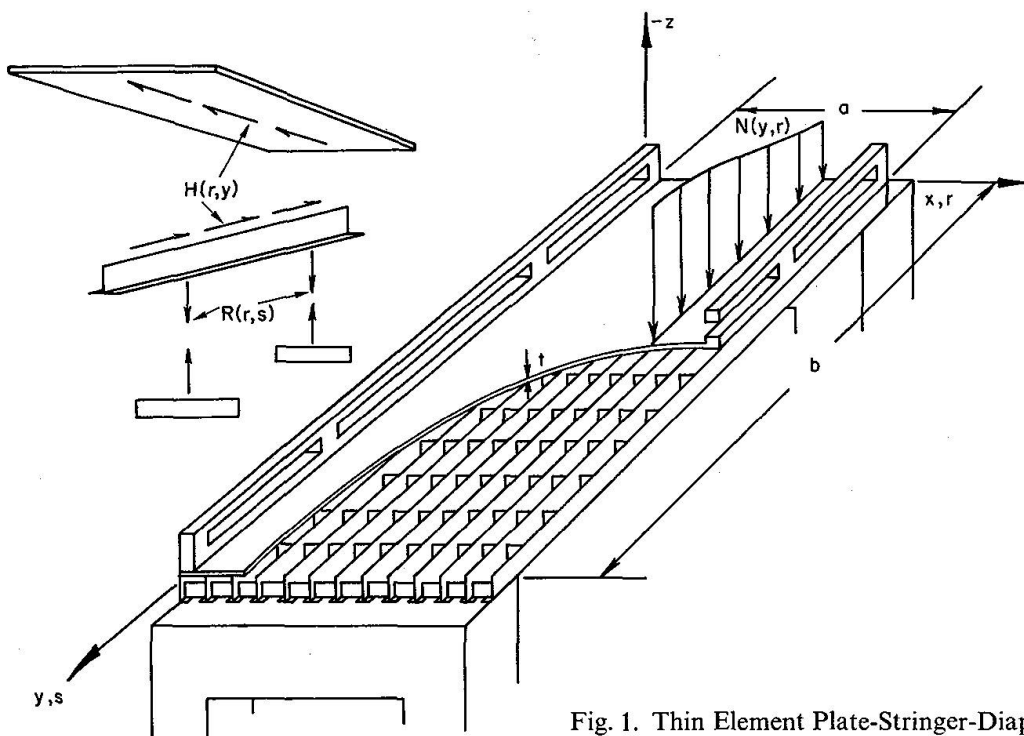

Fig. 1. Thin Element Plate-Stringer-Diaphragm Deck.

components have negligible out-of-plane stiffness and 2) are simply supported at the ends. Thus, the linear superposition of several solutions is required to analyze decks that are continuous over intermediate supports.

The thin element plate-stringer-diaphragm deck in either cellular or orthotropic form is one of the most efficient load carrying systems employed by designers today and the literature includes many references to recommended methods of analysis. However, none of the existing methods are rationally based even though some are rather complex and require voluminous computations. The present methods of analysis fall into three categories, 1) use of totally empirical design formulas to compute an "effective flange width" and the distribution of loads between the resulting "T" beam stringers (8); 2) use of a "smearing out" technique to replace the mixed discrete-continuous system by an "equivalent" (usually orthotropic) continuum (5, 9) and 3) use of a discrete or latticed system to approximate the real system through a finite difference or finite element approach (1, 7).

The "equivalent continuum" method is attractive in that a single continuum solution can be used for preliminary design studies of a variety of discrete-continuous deck systems; however, the steps of selecting the substitute continuum and interpreting the results for the real system lack rational bases and introduce significant errors for coarse lattices and those closely stiffened decks with relatively stiff ribs. Also, the solution for the approximate continuous model is often more difficult and less elegant than the solution for the exact discrete-continuous model.

Of the various substitute lattice approaches the finite element method is currently the most popular and canned programs are available for office use; however, their use for numerous alternate designs is quite expensive due to the voluminous computations and the extensive input data required for each case. Furthermore the state of the art of error analysis for this method is not sufficiently well developed to insure against errors which are orders of magnitude larger than predicted. One example of such a situation is the case of a deck with stiff ribs and a flexible plate so that the higher harmonics contribute significantly to the deflection field. In such a case it is extremely difficult to get a meaningful stress analysis via a finite element approach.

The concept of deriving exact formulas for the elastic analysis of reinforced bridge decks is not entirely new as both the micro discrete field approach (i.e. use of difference equation models) (2) and the macro discrete field approach (i.e. use of summation equation models) (3, 4) have been used for the rational analysis of ribbed plates or decks composite with supporting stringers. This paper extends the use of the macro approach to thin plates supported by both stringers and diaphragms and thus covers the more general concept of an orthotropic deck.

It is proposed that the exact elastic analysis presented herein be used for final design review. (While the formulas may be considered complex for manual computations, they can be conveniently employed through the use of a small computer or one of the several programmable electronic desk calculators that have recently come on the market). A secondary goal is to make available a standard analysis for use in studying existing and proposed approximate formulas in order to establish range of applicability, magnitude of errors, etc. This should obviate the unsatisfactory practice of making judgements based upon comparison of one empirical method with another empirical method.

The major results are numerically illustrated through use of the formulas for the analysis of realistic structures. One bridge is also analyzed by a finite element method for comparative purposes.

Mathematical Model

A macro discrete field approach (3) is used to find the in-plane interactive forces, $H(r, y)$, between the stringers and the plate and the out-of-plane interactive forces, $R(r, s)$, between the stringers and the diaphragms (see Fig. 1). The macro approach is dictated by the fact that an analysis of the entire top plate is tractable for a general loading due to the simple end support conditions at $y = 0$ and b. A rational micro discrete field approach, on the other hand, is not possible as it requires the general boundary solution for a typical rectangular plate element, between two successive stringers and diaphragms, which is unavailable.

The solutions for continuous and discrete deflection or force fields are found in terms of infinite and finite sinusoidal series, respectively. For example the unknown horizontal interactive forces between the top of the stringers and the plate is expressed as follows:

$$H(r,y) = \sum_{j=1}^{\infty} \sum_{k=1}^{m-1} H_{kj} \sin \frac{k\pi r}{m} \cos \overline{\alpha}_j y \qquad (1)$$

$$H_{kj} = \frac{4}{mb} \sum_{r=1}^{m-1} \int_0^b H(r, y) \sin \frac{k\pi r}{m} \cos \overline{\alpha}_j y \, dy \qquad (2)$$

in which $\overline{\alpha}_j = \frac{j\pi}{b}$ and $r = 1, (1), m - 1$.

The continuous plate deflections can be found in terms of the unknown stringer plate interactive forces as follows:

$$u(x,y) = u^h(x,y) + \sum_{\alpha=1}^{m-1} \int_0^b H(\alpha, \eta) \, K^{uy}(x, y, \tfrac{a}{m} \alpha, \eta) d\eta \qquad (3)$$

$$v(x, y) = v^h(x, y) + \sum_{\alpha=1}^{m-1} \int_0^b H(\alpha, \eta) \, K^{vy}(x, y, \tfrac{a}{m} \alpha, \eta) d\eta \qquad (4)$$

in which K^{uy} and K^{vy} are the kernel functions for u and v respectively due to a unit inpulse load in the y direction on the plate with simple edge supports (see Eqs. A-2-5) and u^h and v^h are the homogeneous solutions due to the side boundary displacements $v^h(\tfrac{o}{a}, y)$ (see Eqs. A-8-13).

Substitution of Eqs. A-2, A-3, A-8, and A-9 and use of the relation given in Eq. 2, gives the following series for the continuous plate displacements in terms of the boundary displacement coefficients $\overline{V}_{ij}$ and the interactive force coefficients H_{kj}:

$$u(x,y) = \sum_{j=1}^{\infty} \sum_{i=0}^{\infty} (\tfrac{4}{a} \overset{*}{\phi}_i \, \overline{V}_{ij} \overset{*}{A}_{ij} + \tfrac{m}{a} H_{ij} \overset{*}{A}_{ij}) \cos \alpha_i x \sin \overline{\alpha}_j y \qquad (5)$$

$$v(x,y) = \sum_{j=1}^{\infty} \sum_{i=1}^{\infty} (\tfrac{4}{a}\, \overline{V}_{ij}\, \overset{*}{\overline{B}}_{ij} + \tfrac{m}{a}\, H_{ij}\, \overset{*}{B}_{ij}) \sin \alpha_i x \cos \overline{\alpha}_j y \qquad (6)$$

in which H_{ij} is sine wise cyclic, having a period of $2m$, with respect to the first index and the coefficients A_{ij}, B_{ij}, $\overline{A}_{ij}$ and $\overline{B}_{ij}$ are given by Eqs. A-4, A-5, A-12 and A-7 respectively. The stringer line displacements $v(r,y)$ can be expressed as a mixed finite-infinite series thru use of Eq. A-17 with the following results:

$$v(r,y) = \sum_{j=1}^{\infty} \sum_{k=1}^{m-1} [\tfrac{4}{m}\, \overline{V}_{kj}\, \overline{B}_{kj} + H_{kj}\, B_{kj}] \sin \tfrac{k\pi r}{m} \cos \overline{\alpha}_j y \qquad (7)$$

in which B_{kj}, and $\overline{B}_{kj}$ are given by Eqs. A-23, and A-24 respectively.

The stringer and diaphragm deflections depend upon the out-of-plane plate loads, $N(r,y)$, which are applied along the stringer lines, and the out-of-plane stringer-diaphragm interactive node forces, $R(r,s)$, as well as the in-plane plate-stringer interactive forces $H(r,y)$. The series expression for these additional quantities are:

$$N(r,y) = \sum_{j=1}^{\infty} \sum_{k=1}^{m-1} N_{kj} \sin \tfrac{k\pi r}{m} \sin \overline{\alpha}_j y \qquad (8)$$

$$N_{kj} = \tfrac{4}{mb} \sum_{r=1}^{m-1} \int_0^b N(r,y) \sin \tfrac{k\pi r}{m} \sin \overline{\alpha}_j y\, dy \qquad (9)$$

$$R(r,s) = \sum_{l=1}^{n-1} \sum_{k=1}^{m-1} R_{kl} \sin \tfrac{k\pi r}{m} \sin \tfrac{l\pi s}{n} \qquad (10)$$

$$R_{kl} = \tfrac{4}{mn} \sum_{s=1}^{n-1} \sum_{r=1}^{m-1} R(r,s) \sin \tfrac{k\pi r}{m} \sin \tfrac{l\pi s}{n} \qquad (11)$$

The series for the in-plane and out-of-plane displacements at the tops of the interior stringers can now be written as follows:

$$v(r,y) = \sum_{j=1}^{\infty} \sum_{k=1}^{m-1} [\overset{*}{D}_j\, N_{kj} - \overset{*}{B}_j\, H_{kj} - \tfrac{n}{b}\, \overset{*}{D}_j\, R_{kj}] \sin \tfrac{k\pi r}{m} \cos \overline{\alpha}_j y \qquad (12)$$

$$w(r,y) = \sum_{j=1}^{\infty} \sum_{k=1}^{m-1} [\overset{*}{A}_j\, N_{kj} - \overset{*}{D}_j\, H_{kj} - \tfrac{n}{b}\, \overset{*}{A}_j\, R_{kj}] \sin \tfrac{k\pi r}{m} \sin \overline{\alpha}_j y \qquad (13)$$

in which $r = 1$, (1), $m - 1$, $0 \le y \le b$, $\overset{*}{A}_j$, $\overset{*}{B}_j$ and $\overset{*}{D}_j$ are given by Eq. A-27 and R_{kj} is sinewise cyclic on j with a period of $2n$ i.e. $R_{kl} = R_{k,\,2Jn+l} = -R_{k,\,2Jn-l}$ for integer values of J.

The double finite series for the out-of-plane stringer node deflections is found by use of Eq. A-17 as follows:

$$w(r,s) = \sum_{l=1}^{n-1} \sum_{k=1}^{m-1} [W_{kl}^N - W_{kl}^H - A_l\, R_{kl}] \sin \tfrac{k\pi r}{m} \sin \tfrac{l\pi s}{n} \qquad (14)$$

in which $r = 1$, (1), $m - 1$, $s = 0$, (1), n, A_l is given by Eq. A-29

$$W_{kl}^{N} = \sum_{J=-\infty}^{+\infty} \overset{*}{A}_{2Jn+l}\, N_{k,2Jn+l} \simeq \overset{*}{A}_{l}\, N_{kl} \qquad (15\,\mathrm{a,b})$$

$$W_{kl}^{H} = \sum_{J=-\infty}^{+\infty} \overset{*}{D}_{2Jn+l}\, H_{k,2Jn+l} \simeq \overset{*}{D}_{l}\, H_{kl} \qquad (16\,\mathrm{a,b})$$

The out-of-plane node deflections of the diaphragms depend upon the out-of-plane side boundary deflections as well as the stringer-diaphragm interactive forces.

$$w(\tfrac{0}{a}, y) = \sum_{j=1}^{\infty} (W_j^{\$} \pm W_j^{q/s}) \sin \bar\alpha_j y \qquad (17)$$

$$w(r,s) = \sum_{l=1}^{n-1} \sum_{k=1}^{m-1} [C_k\, \overline{W}_{kl}^{f} + A_k^{d}\, R_{kl}] \sin \tfrac{k\pi r}{m} \sin \tfrac{l\pi s}{n} \qquad (18)$$

in which $r = 1$, (1), $m - 1$, $s = 0$, (1), n, A_k^{d} is the discrete kernel function coefficient for a typical diaphragm, similar to Eq. A-29 for stringers, i.e.

$$A_k^{d} = \frac{1}{12 B^{d}} \left(\tfrac{a}{m}\right)^3 \frac{3 - \sigma_k}{(\sigma_k)^2}; \qquad \sigma_k = 1 - \cos \tfrac{k\pi}{m} \qquad (19\,\mathrm{a,b})$$

and B^{d} equals the flexural rigidity of the diaphragm.

$$\overline{W}_{kl}^{f} = \sum_{J=-\infty}^{+\infty} \overline{W}_{k,2Jn+l} \qquad (20\,\mathrm{a})$$

$$\overline{W}_{kj} = \begin{bmatrix} W_j^{\$} & \text{for } k \text{ odd} \\ W_j^{q/s} & \text{for } k \text{ even} \end{bmatrix} \qquad (20\,\mathrm{b})$$

$$1 = \sum_{k=1,3,\ldots}^{m-1} C_k \sin \tfrac{k\pi r}{m}; \qquad 1 - 2\tfrac{r}{m} = \sum_{k=2,4,\ldots}^{m-1} C_k \sin \tfrac{k\pi r}{m} \qquad (21\,\mathrm{a,b})$$

$$C_k = \tfrac{2}{m} \cot \tfrac{k\pi}{2m} \qquad (21\,\mathrm{c})$$

The relations developed thus far are sufficient for the analysis of a deck system or orthotropic panel with known side boundary displacements, e.g. $\overline{V}_{kj} = \overline{W}_{kj} = 0$; however for the typical bridge deck one usually has to determine the side boundary displacements so as to establish compatibility with the boundary stringers, which have physical properties denoted by B^{b}, e^{b} and ρ^{b} and may be loaded as follows:

$$N(\tfrac{0}{m}, y) = \sum_{j=1}^{\infty} (P_j^{\$} \pm P_j^{q/s}) \sin \bar\alpha_j y \qquad (22)$$

The compatibility of boundary stringer and deck boundary displacements can be established by expressing the boundary stringer displacements in terms of their

applied loads plus the loads transferred to them by deck action. For example, consider the stringer at $r = 0$

$$v(0, y) = \int_0^b \left[P^t(0, \eta) \, K_b^{vz}(y, \eta) + T^t(0, \eta) \, K_b^{vy}(y, \eta) \right] d\eta \tag{23}$$

$$w(0, y) = \int_0^b \left[P^t(0, \eta) \, K_b^{wz}(y, \eta) + T^t(0, \eta) \, K_b^{wy}(y, \eta) \right] d\eta \tag{24}$$

in which the coefficients of K_b^{vz}, K_b^{vy}, K_b^{wz}, and K_b^{wy} are as given by Eq. A-27 except that all the interior stringer descriptors, $\overset{*}{B}$, $\overset{*}{e}$, and $\overset{*}{\rho}$, are replaced by boundary stringer descriptors, B^b, e^b and ρ^b to get $\overset{*}{A}{}_j^b$, $\overset{*}{B}{}_j^b$ and $\overset{*}{D}{}_j^b$. The quantities $P^t(0, \eta)$ and $T^t(0, \eta)$ represent total out-of-plane or transverse and in-plane or longitudinal load components applied to the boundary stringer from all effects. That is,

$$P^t(0, y) = N(0, y) + \sum_{\alpha = 1}^{m-1} \sum_{\beta = 1}^{n-1} R(\alpha, \beta)(1 - \tfrac{\alpha}{m}) \delta(y - \tfrac{b}{n}\beta) \tag{25}$$

$$T^t(0, y) = n_{xy}^h(0, y) + \sum_{\alpha = 1}^{m-1} \int_0^b H(\alpha, \eta) \, K^{Ty}(0, y, \tfrac{a}{m}\alpha, \eta) \, d\eta \tag{26}$$

or carrying out the indicated operations

$$P^t(0, y) = \sum_{j=1}^{\infty} \left[(P_j^\$ + P_j^{a/s}) + \tfrac{mn}{4b} \sum_{k=1}^{m-1} C_k \, R_{kj} \right] \sin \overline{\alpha}_j y \tag{27}$$

$$T^t(0, y) = \sum_{j=1}^{\infty} \left[(\overline{T}_j^\$ \, V_j^\$ + \overline{T}_j^{a/s} \, V_j^{a/s}) + \sum_{k=1}^{m-1} \overline{B}_{kj} \, H_{kj} \right] \cos \overline{\alpha}_j y \tag{28}$$

in which $\overline{T}_j^\$$ and $\overline{T}_j^{a/s}$ are given by Eq. A-15 and $\overline{B}_{kj}$ is given by Eq. A-24c.

All the necessary relations are now available to complete the mathematical model needed to solve for H_{kj}, R_{kl}, $V_j^\$$ (or $V_j^{a/s}$) and $W_j^\$$ (or $W_j^{a/s}$) as follows: 1) compatibility of in-plane stringer line displacements between the plate and the stringer tops is obtained by equating Eqs. 7 and 12; 2) compatibility of out-of-plane node displacements between the stringers and the diaphragms is obtained by equating Eqs. 14 and 18; 3) compatibility of in-plane boundary displacements is obtained by substituting Eqs. 27 and 28 into Eq. 23; and 4) compatibility of out-of-plane boundary displacements is obtained by substituting Eqs. 27 and 28 into Eq. 24. The resulting model (shown for symmetric component of boundary displacements) is:

$$(B_{kj} + \overset{*}{B}_j) \, H_{kj} + \tfrac{n}{b} \overset{*}{D}_j \, R_{kj} + \tfrac{4}{m} \overline{B}_{kj} \, V_j^\$ = \overset{*}{D}_j \, N_{kj} \tag{29}$$

$$\sum_J \overset{*}{D}_{2Jn+l} \, H_{k, 2Jn+l} + (A_k^d + A_l) R_{kl} + C_k \sum_J W_{2Jn+l}^\$ = \sum_J \overset{*}{A}_{2Jn+l} \, N_{k, 2Jn+l} \tag{30}$$

$$\sum_k \left[\overset{*}{B}{}_j^b \, \overline{B}_{kj} \, H_{kj} + \tfrac{mn}{4b} \overset{*}{D}{}_j^b \, C_k \, R_{kj} \right] + \left[\overset{*}{B}{}_j^b \, \overline{T}_j^\$ - 1 \right] V_j^\$ = - \overset{*}{D}{}_j^b \, P_j^\$ \tag{31}$$

$$\sum_k \left[\overset{*}{D}{}_j^b \, \overline{B}_{kj} \, H_{kj} + \tfrac{mn}{4b} \overset{*}{A}{}_j^b \, C_k \, R_{kj} \right] + \overset{*}{D}{}_j^b \, \overline{T}_j^\$ \, V_j^\$ - W_j^\$ = - \overset{*}{A}{}_j^b \, P_j^\$ \tag{32}$$

in which $J = -\infty$, (1), $+\infty$ with convergence about $J = 0$ and $k = 1$, (2), $m - 1$. To solve for antisymmetric boundary displacements replace all $\$$ quantities by the analogous a/s quantities and use $k = 2$, (2), $m - 1$. It is apparent that this model cannot be dealt with as a set of algebraic equations due to inconformability — i.e. Eq. 29 is for kj indexed quantities, Eq. 30 is for kl indexed quantities and Eqs. 31 and 32 are for j indexed quantities — and the fact that some terms are sums; however, as will be shown in subsequent sections, the simaltaneous equations can be solved by successive elimination of unknowns.

Solution for Simple Side Supports

For the case of a panel or deck with known side boundary deflections, $V_j^\$$ (and/or $V_j^{q/s}$) and $W_j^\$$ (and/or $W_j^{q/s}$), Eqs. 31 and 32 are not needed and one can solve Eqs. 29 and 30 for H_{kj} and R_{kl} in terms of N_{kj}, $V_j^\$$ and $W_j^\$$ by using Eq. 29 to eliminate H_{kj} from Eq. 30 which is then solved for R_{kl}. For example, consider the title case of simple side supports, i.e. $V_j^\$ = V_j^{q/s} = W_j^\$ = W_j^{q/s} = 0$, such as an orthotropic or sandwich panel with relatively rigid supports along all four edges. The exact solution is:

$$H_{kj} = \frac{\overset{*}{D}_j\left(N_{kj} - \frac{n}{b} R_{kj}\right)}{B_{kj} + \overset{*}{B}_j} \tag{33}$$

$$R_{kl} = \frac{W_{kl}^N - A_{kl}^N}{A_l + A_k^d - \frac{n}{b} \overline{A}_{kl}^R} \tag{34}$$

in which $\overset{*}{B}_j$ and $\overset{*}{D}_j$ are given by Eq. A-27; A_l and A_k^d are given by Eqs. A-29 and 20; B_{kj} is given by Eq. A-24; W_k^{Nl} is given by Eq. 15; R_{kj} is sinewise cyclic on j with a period of $2n$; and the two special terms A_{kl}^N and $\overline{A}_{kl}^R$ are:

$$A_{kl}^N = \sum_{J=-\infty}^{+\infty} \frac{(\overset{*}{D}_{2Jn+l})^2 N_{k, 2Jn+l}}{B_{k, 2Jn+l} + \overset{*}{B}_{2Jn+l}} \simeq \frac{(\overset{*}{D}_l)^2 N_{kl}}{B_{kl} + \overset{*}{B}_l} \tag{35a,b}$$

$$\overline{A}_{kl}^R = \sum_{J=-\infty}^{+\infty} \frac{(\overset{*}{D}_{2Jn+l})^2}{B_{k, 2Jn+l} + \overset{*}{B}_{2Jn+l}} \simeq \frac{(\overset{*}{D}_l)^2}{B_{kl} + \overset{*}{B}_l} \tag{36a,b}$$

It should be noted that for the simply supported panel each "k" (first index) load harmonic yields a single "k" solution harmonic but the effect of a j (second index) loading harmonic is different due to action of the diaphragms; i.e. each "j" loading harmonic yields 1) a single finite series "l" solution harmonic, whose relation to "j" is through $l = j - 2Jn$ or $2Jn - j (l < n)$ and 2) an infinite set of "j" solution harmonics related to j through $j' = 2Jn \pm j$.

An accurate approximate solution for H_{kj} and R_{kl}, which contains only algebraic terms, can be written by consistently truncating all the transformation series after the first term. (e.g. use $J = 0$ only so that Eqs. 35b and 36b are used instead of 35a and 26a). The accuracy of such a rational approximation increases as the

numbers of stringers, $m - 1$, and diaphragms, $n - 1$, increases. The result of this simplification of Eqs. 33 and 34 is:

$$H_{kj} \simeq \frac{\left(\dfrac{e}{\bar{\alpha}_j}\right)(N_{kj} - \frac{n}{b} R_{kj})}{e^2 + \bar{\rho}^2_{kj}} \tag{37}$$

$$R_{kl} \simeq \frac{\frac{b}{n} N_{kl}}{1 + \psi_{kl}\left[\dfrac{e^2 + \bar{\rho}^2_{kl}}{\bar{\rho}^2_{kl}}\right]} \tag{38}$$

$$\bar{\rho}^2_{kj} = \rho^2 + \left(\tfrac{mB}{aK}\right)\left(\tfrac{ja}{kb}\right)^2 \frac{\frac{2}{1-\mu} + \left(\tfrac{ja}{kb}\right)^2}{\left[1 + \left(\tfrac{ja}{kb}\right)^2\right]^2} \tag{39}$$

$$\psi_{kl} = \left(\tfrac{la}{kb}\right)^4 \left(\frac{mbB}{naB^d}\right) \tag{40}$$

These approximate formulas for H_{kj} and R_{kl} can be evaluated manually in less than 10 minutes.

Numerical Example 1

In order to illustrate the numerical use of the above solutions for a simply supported thin element plate-stringer-diaphragm system, consider a panel (similar to Fig. 1 except simply supported, on the sides as well as the ends) with physical data as follows:

$a = 144$ in.; $b = 72$ in, $m = 12$, $n = 4$, $t = .125$, $\mu = .3$, $E = 29{,}000$ ksi, $B = \frac{5}{3} E$ kip/in.^{2}, $e = 2.0$ in., $\rho^2 = \frac{4}{3}$ in.^{2}; and $B^d = \frac{40}{3} E$ kip. in.^{2}. The out-of-plane stringer line load is harmonic; i.e. $N_{11} = .01$ kip/in. All other $N_{kj} = 0$ or $N(r,y) = (.01) \sin \frac{\pi r}{m} \sin \frac{\pi y}{b}$. Some of the intermediate results are: $\overset{*}{A}_1 = 5.7080$ in.^{2}/kip, $\overset{*}{B}_1 = .05796$ in.^{2}/kip, $\overset{*}{D}_1 = .49812$ in.^{2}/kip (Eq. A-27); $W^N_{11} = .05708$ in. (Eq. 15a); $A_1 = .3173$ in./kip (Eq. A-29) or $A_1 \simeq .3171$ in./kip (Eq. A-28b); $A^d_1 = .95134$ in./kip (Eq. 19); $K = 3983.5$ kip/in. (Eq. A-1); $\overset{*}{B}_{1,1} = .14466$ in.^{3}/kip (Eq. A-5); $B_{1,1} = .012770$ in.^{2}/kip (Eq. A-23c) or $B_{1,1} \simeq .01205$ in.^{2}/kip (Eq. A-23b); $A^N_{11} = .03508$ in. (Eq. 35a); $\overline{A}^R_{11} = 3.5096$ in.^{2}/kip (Eq. 36a) or $\overline{A}^R_{11} \simeq 3.5081$ in.^{2}/kip (Eq. 36b); $R_{11} = .0204897$ kip. Other $R_{kl} = 0$ (Eq. 34) or $R_{11} \simeq .0202$ kip (Eq. 38); and $H_{11} = .062410$ kip/in., $H_{1,7} = .000851$ kip/in., $H_{1,9} = -.000590$ kip/in., $H_{1,15} = .000268$ kip/in. and $H_{1,17} = -.000219$ kip/in. (Eq. 33) or $H_{11} \simeq .06316$ kip/in. (Eq. 37). These intermediate results were used in the deflection field equations with the following results (inch units): The out-of-plane node deflections (Eq. 19 with $\overline{W}^f_{kl} = 0$) are

$$w(r,s) = (.019493) \sin \tfrac{\pi r}{m} \sin \tfrac{\pi y}{b}.$$

The out-of-plane stringer line deflections (Eq. 13) are

$$w(r,y) = (.019495) \sin \tfrac{\pi r}{m} \left[\sin \tfrac{\pi y}{b} + .000075 \sin \tfrac{7\pi y}{b} - .000030 \sin \tfrac{9\pi y}{b} + .000004 \sin \tfrac{15\pi y}{b} - .000003 \sin \tfrac{17\pi y}{b} + ...\right]$$

The in-plane stringer line deflections (Eq. 12 or Eq. 7) with $\overline{V}_{kj} = 0$) are:

$$v(r,y) = (7.9695 \times 10^{-4}) \sin \tfrac{\pi r}{m} \left[\cos \tfrac{\pi y}{b} + .00081 \cos \tfrac{7\pi y}{b}\right.$$
$$\left. - .00045 \cos \tfrac{9\pi y}{b} + .00012 \cos \tfrac{15\pi y}{b} - .00009 \cos \tfrac{17\pi y}{b} + ...\right]$$

and the continuous in-plane plate deflections (Eq. 6 with $\overline{V}_{ij} = 0$) are:

$$v(x,y) = (7.5238 \times 10^{-4}) \sin \tfrac{\pi x}{a}\left[\cos \tfrac{\pi y}{b} + .00025 \cos \tfrac{7\pi y}{b} + .00011 \cos \tfrac{9\pi y}{b} + ...\right]$$
$$- (.1463 \times 10^{-4}) \sin \tfrac{23\pi x}{a} \cos \tfrac{\pi y}{b} + (.12408 \times 10^{-4}) \sin \tfrac{25\pi x}{a} \cos \tfrac{\pi y}{b} + ...$$

Note that convergence is rapid even for this case of a relatively small number of diaphragms, $n = 4$.

Analysis of Cellular Decks

As mentioned in the introduction, formulas for the exact elastic analysis of an orthotropic deck can also be used for the analysis of cellular decks that are symmetric about the middle plane, i.e. the top and bottom plates have equal thicknesses. All that is required is to modify the input data for an orthotropic deck so as to produce a condition of anti-symmetry with respect to the middle plane as follows: 1) use only the antisymmetric component of the top and bottom stringer line loads (the symmetric component only squeezes the stringers and can be ignored); 2) use one half the actual flexural rigidity of the stringers B and B^b, and diaphragms, B^d; and 3) use radius of gyration, ρ and ρ^b equal to zero (or if stringer representation is flexural rigidity and cross sectional area use an area approaching infinity).

Numerical Example 2

In order to briefly illustrate modification of data for the analysis of a cellular planel, consider the investigation of a cellular design alternative to example 1 using the same amount of material; i.e., same stringers and diaphragms but two 1/16 in. plates instead of a single 1/8 in. plate. For this case, the input data are $a = 144$ in., $b = 72$ in., $m = 12$, $n = 4$, $t = .0625$ in. $\mu = .3$, $E = 29000$ ksi., $B = \tfrac{5}{6}\, E$ kip/in.^{2}, $e = 2.0$ in., $\rho^2 = 0$, $B^d = \tfrac{2Q}{3}\, E$ kip/in.^{2} and $N_{11} = .005$ kip/in. (other $N_{kj} = 0$). The calculations are too similar to those for Example 1 to warrant showing detailed results, but a design comparison can be made by showing the out-of-plane node deflections as follows:

$$w(r,s) = (.01205) \sin \tfrac{\pi r}{m} \sin \tfrac{\pi s}{n}$$

That is, the cellular construction gives a 62% stiffer panel with the same amount of material.

Solution for Flexible Side Supports

The most general case considered in this paper is that of an orthotropic deck with flexible side supports. The two identical boundary stringers are of an arbitrary size and shape with arbitrary loads. The analysis allows for possibility that the boundary stringers are also composite with the deck plate, but detailing for non-composite action can be dealt with by setting the boundary stringer eccentricity, e^b, equal to zero. For this general case, one must solve Eqs. 29-32 for H_{kj}, R_{kl}, $V_j^\$$ (or $V_j^{q/s}$) and $W_j^\$$ (or $W_j^{q/s}$) in terms of the load coefficients N_{kj} and $P_j^\$$ (or $P_j^{q/s}$) This exact elastic model can be formally reduced to a single equation with one unknown by successive elimination as was done with the two equation model for the simple side support case; however, the results for the four equation model are unwieldy and many of the coefficients are sums of obscure physical significance. (Even in the simpler case of simultaneous algebraic equations, it is seldom practical to derive an explicit formula solution for a model with more than three equations). For this model, convergence of the series summed on J is very rapid and indications are that computers, or programmable calculators will normally be used to get numerical results; thus, an alternate procedure is recommended as follows:

1. Truncate the series on H_{kj} and $W_j^\$$ in Eq. 30 after one term (i.e. use $J = 0$ only) and solve Eqs. 29 and 30 simultaneously for H_{kl} and R_{kl} ($l < n$) in terms of N_{kl}, $V_l^\$$ (or $V_l^{q/s}$) and $W_l^\$$ (or $W_l^{q/s}$).

2. Substitute the results of step 1 into Eqs. 31 and 32 solve the resulting algebraic equation for $V_l^\$$ (or $V_l^{q/s}$) and $W_l^\$$ (or $W_l^{q/s}$).

3. Substitute results of step 2 into the results of step 1 to find H_{kl} and R_{kl}.

4. Use the cyclic properties of R_{kj} (e.g. $R_{kl} = R_{k, 2n+l} = R_{k, l-2n}$) to solve Eqs. 29 and 31 for the higher harmonics of H_{kj} and $V_j^\$$ ($j > n$) and then substitute into Eq. 32 to find the higher harmonics of $W_j^\$$. (That is, first use Eq. 29 to eliminate H_{kj} from Eq. 31 and solve for $V_j^\$$ (or $V_j^{q/s}$). Then find H_{kj} from Eq. 29 and, in turn, $W_j^\$$ from Eq. 32).

5. If unusual accuracy is required, retain additional terms in the summations of H_{kj} and $W_j^\$$ in Eq. 30 ($J = -2$ to $+2$ is sufficient), solve for improved results for R_{kl} and repeat step 4. (In most cases, the results obtained in step 4 on the initial cycle are sufficiently accurate so that step 5 can be omitted).

This completes the algorithm for the general case of flexible side supports. Note that the effects of the side boundary deflections invalidate the one-to-one relation between the "k" loading and solution harmonics that existed for the case of simple side supports. For example, a single "k odd" loading harmonic will normally cause a deflection field with series coefficients containing all possible k odd harmonics. The relation between the "j" (second index) loading and solution harmonics is as described in the section on simple side supports.

Numerical Example 3

In order to illustrate numerical use of the general bridge deck formulas under loading conditions which place a severe test on the convergence of the solution series, consider a bridge with the following physical parameters and loading:

$a = 360$ in., $b = 720$ in.; $m = 12$; $n = 4$; $t = .375$ in.; $\mu = .29$; $E = 29000$ ksi; $B = B^b = 10.2681 \times 10^6$ kip in.^{2}; $e = e^b = 14.4286$ in., $\rho = \rho^b = 5.807$ in. and $B^d = 8.41 \times 10^6$ kip in.^{2}. The loading consists of two symmetrically placed 20 kip concentrated loads, i.e. $N(r,y) = 20(\delta_r^5 + \delta_r^7)\ \delta(y - \frac{b}{2})$ or $N_{kj} = \frac{8P}{mb}\ (-1)^{\frac{k-1}{2}}$ $(-1)^{\frac{j-1}{2}} \cos \frac{k\pi}{m}(k$ and j odd only) and $P_j^\$ = P_j^{q\$} = 0$. The combination of a relatively small number of stringers and diaphragms and loads of ·infinite intensity tend to show a harmonic analysis in a poor light due to slow convergence; however, as the results below indicate, even for this case the convergence is quite good, yielding practical results after only a small numbers of terms.

Some of the intermediate results are:

$\overset{*}{K} = 11,873.$ kip/in. (Eq. A-1); $\overset{*}{A}_1 = 268.68$ in.^{2}/kip, $\overset{*}{B}_1 = 1.2374$ in.^{2}/kip and $\overset{*}{D}_1 = 16.915$ in.^{2}/kip (Eq. A-27); $B_{11} = 0.07295$ in.^{2}/kip (Eq. A-23); $W_{11}^N = 4.8088$ in. (Eq. 15); $A_1 = 1.494$ in./kip., (Eq. A-29) $.A_1^d = .6834$ in./kip. (Eq. 19); $\overline{B}_{11} = 2.2456$ (Eq. A-24); and $\overline{T}_1^\$ = -26.179$ ksi (Eq. A-15). $V_1^\$ = .01530$ in., $W_1^\$ = .2818$ in. (step 2 of algorithm p. 52); $H_{11} = .1705$ kip/in., $R_{11} = .7203$ kip (step 3 of algorithm p. 52); $V_7^\$ = -1.123 \times 10^{-5}$ in., $H_{17} = -.02362$ kip/in., $W_7^\$ = -5.213 \times 10^{-5}$ in., (step 4 of algorithm p. 52); $R_{11} = .7195$ kip (step 5 of algorithm p. 52 which confirms that recycling is unnecessary).

The deflection fields are as follows:

$v(r,y) = [23.97 \cos \frac{\pi y}{b} - 1.318 \cos \frac{3\pi y}{b} + .2976 \cos \frac{5\pi y}{b} + ...]10^{-3} \sin \frac{\pi r}{m} + [5.774 \cos \frac{\pi y}{b} + .7076 \cos \frac{3\pi y}{b} - .1253 \cos \frac{5\pi y}{b} + ...]10^{-3} \sin \frac{3\pi r}{m} + [3.261 \cos \frac{\pi y}{b} + .01996 \cos \frac{3\pi y}{b} - .00567 \cos \frac{5\pi y}{b} + ...]10^{-3} \sin \frac{5\pi r}{m} + ...$

$w(r,y) = [848.0 \sin \frac{\pi y}{b} - 14.20 \sin \frac{3\pi y}{b} + 1.876 \sin \frac{5\pi y}{b} + ...]10^{-3} \sin \frac{\pi r}{m} + [92.89 \sin \frac{\pi y}{b} + 7.133 \sin \frac{3\pi y}{b} - .8491 \sin \frac{5\pi y}{b} + ...]10^{-3} \sin \frac{3\pi r}{m} + [62.07 \sin \frac{\pi y}{b} - .1742 \sin \frac{3\pi y}{b} + .01886 \sin \frac{5\pi y}{b} + ...]10^{-3} \sin \frac{5\pi r}{m} + ...$

The membrane stress resultant field, n_y, (from Eq. A-1) is

$n_y(x,y) = -K\{[.0944 \sin \frac{\pi y}{b} - .01433 \sin \frac{3\pi y}{b} + .005499 \sin \frac{5\pi y}{b} + ...]10^{-3} \sin \frac{\pi x}{a} + [.02460 \sin \frac{\pi y}{b} + .003893 \sin \frac{3\pi y}{b} - .002209 \sin \frac{5\pi y}{b} + ...]10^{-3} \sin \frac{3\pi x}{a} + [.01533 \sin \frac{\pi y}{b} + .00067 \sin \frac{3\pi y}{b} - .000239 \sin \frac{5\pi y}{b} + ...]10^{-3} \sin \frac{5\pi x}{a} + ...$

The membrane stress resultant, n_y, at the center of the deck $(x = \frac{a}{2}, y = \frac{b}{2})$ is $n_y = 1.293$ kips/in. The finite element analysis described in the next section yields a stress $n_y = 1.179$, 1.192 or 1.419 kips/in. depending upon type of element utilized.

Comparison with Alternative Approaches

For comparative purposes the bridge system analyzed for Example 3 was also analyzed by use of a more comprehensive theoretical model and by use of discretized or finite element model.

The more comprehensive theoretical model was one which included the out-of-plane stiffness or flexural actions of the deck plate as well as its inplane stiffness. The composite membrane-flexural model treated $N(r,y)$ as an unknown out-of-plane interactive force between the stringers and the plate and rationally accounted for the effects of deck loads applied between stringers. The computations were

thus complicated considerably but gave essentially the same deflection field, for example the maximum difference for $w(r, y)$ was 2.3% which confirmed the authors' hypothesis that the composite membrane model (Eqs. 29-32) is sufficiently sophisticated to analyze metal deck bridges of orthotropic design.

There was also some question as to the need for a rational theoretical analysis in view of the availability of various open form finite element programs which can be modified to approximately model such decks. A space frame program (for the stringers, diaphragms and pseado stud members of length e to model composite action) was combined with a finite element plane stress program (using elements whose width equaled the stringer spacing and length equaled ⅓ the diaphragm spacing) to analyze the deck as an "equivalent" framework. Even though double symmetry was utilized, this relatively coarse network required two orders of magnitude more computing time than did the formula approach (which incidently was written to give research accuracy rather than computational efficiency) and, of more significance, required nearly three orders of magnitude more input information (only one card is needed to read in data for the theoretical approach). The finite element results were in error by up to 10% for deflections and the plate stress distributions bore little resemblance to the exact results. The need for rationally based formulas appeared to be confirmed.

Conclusions

Formulas were introduced which provide the designer with an exact elastic analysis of thin element bridge decks consisting of a set of evenly spaced stringers that are composite with a rectangular plate and are braced by a set of evenly spaced diaphragms. The system is simply supported at the ends with simple or flexible side supports. The loading consists of an arbitrary distribution of stringer line loads. The solution is readily modified to analyze cellular decks or, through superposition, decks with intermediate supports.

The formulas are simple enough for manual use if the loading can be adequately represented by one or two sinusoidal harmonics but in most cases the designer will probably prefer to use a small programmable calculator or a computer. Additional work using these exact formulas seems indicated to modify and determine applicable range for the various empirical formulas presently in use and possibly to point the way toward a more accurate finite element analysis.

Acknowledgments

Reference Formules

Membrane Analysis. — Certain formulas from the classical plane stress elasticity solution for a rectangular plate subjected to in-plane loads and boundary displacements (see Fig. A-1) are needed to account for composite action between the plate and stringers.

The membrane stress resultants, in terms of in-plane displacements, are:

$$\begin{bmatrix} n_x(x,y) \\ n_{xy}(x,y) \\ n_y(x,y) \end{bmatrix} = K \begin{bmatrix} D_x & \mu D_y \\ \frac{1-\mu}{2} D_y & D_y & \frac{1-\mu}{2} D_x \\ \mu D_x & D_y \end{bmatrix} \begin{bmatrix} u(x,y) \\ v(x,y) \end{bmatrix} \tag{A-1}$$

in which D denotes differentiation with respect to the indicated variable, μ equals poissons ratio and $K = Et/(1 - \mu^2)$.

The kernel function solutions for the u and v displacements due to a unit concentrated load in y direction are:

$$K^{uy}(x,y,\xi,\eta) = \frac{4}{ab} \sum_{j=1}^{\infty} \sum_{i=1}^{\infty} \overset{*}{A}_{ij} \sin \alpha_i \xi \cos \overline{\alpha}_j \eta \cos \alpha_i x \sin \overline{\alpha}_j y \tag{A-2}$$

$$K^{vy}(x,y,\xi,\eta) = \frac{4}{ab} \sum_{j=0}^{\infty} \sum_{i=1}^{\infty} \overset{*}{\phi}_j \overset{*}{B}_{ij} \sin \alpha_i \xi \cos \overline{\alpha}_j \eta \sin \alpha_i x \cos \overline{\alpha}_j y \tag{A-3}$$

in which $\alpha_i = \frac{i\pi}{a}$, $\overline{\alpha}_j = \frac{j\pi}{b}$, $\overset{*}{\phi}_j = 1 - \frac{1}{2} \delta_j^0$.

$$\overset{*}{A}_{ij} = \left(\frac{-1}{K} \right) \frac{(1+\mu) \alpha_i \overline{\alpha}_j}{(1-\mu)(\alpha_i^2 + \overline{\alpha}_j^2)^2} \tag{A-4}$$

$$\overset{*}{B}_{ij} = \frac{1}{K} \frac{2\alpha_i^2 + (1-\mu)\overline{\alpha}_j^2}{(1-\mu)(\alpha_i^2 + \overline{\alpha}_j^2)^2} \tag{A-5}$$

It should be noted that the displacement kernel functions K^{uy} and K^{vy} are for a plate that is simply supported along all four edges i.e. $u(x, \overset{0}{b}) = n_y(x, \overset{0}{b}) = 0$ and $v(\overset{0}{a}, y) = n_x(\overset{0}{a}, y) = 0$.

The in-plane membrane shear, n_{xy}, due to the above impulse loading is:

$$K^{Ty}(x,y,\xi,\eta) = \frac{4}{ab} \sum_{j=0}^{\infty} \sum_{i=1}^{\infty} \overset{*}{\phi}_j \overset{*}{B}_{ij} \sin \alpha_i \xi \cos \alpha_j \eta \cos \alpha_i x \cos \overline{\alpha}_j y \tag{A-6}$$

$$\overset{*}{B}_{ij} = \frac{\alpha_i(\alpha_i^2 - \mu \overline{\alpha}_j^2)}{(\alpha_i^2 + \overline{\alpha}_j^2)^2} \tag{A-7}$$

The homogeneous membrane solutions due to known boundary displacements are:

$$v^h(\overset{0}{a}, y) = \sum_{j=1}^{\infty} (V_j^s \pm V_j^{a/s}) \cos \overline{\alpha}_j y \tag{A-8}$$

$$v^h(x,y) = \frac{4}{a} \sum_{j=1}^{\infty} \sum_{i=1}^{\infty} \overline{V}_{ij} \overset{*}{B}_{ij} \sin \alpha_i x \cos \overline{\alpha}_j y \quad 0 < x < a \tag{A-9}$$

$$\overline{V}_{ij} = \begin{bmatrix} V_j^\$ \text{ for } i \text{ odd} \\ V_j^{a/s} \text{ for } i \text{ even} \end{bmatrix}$$

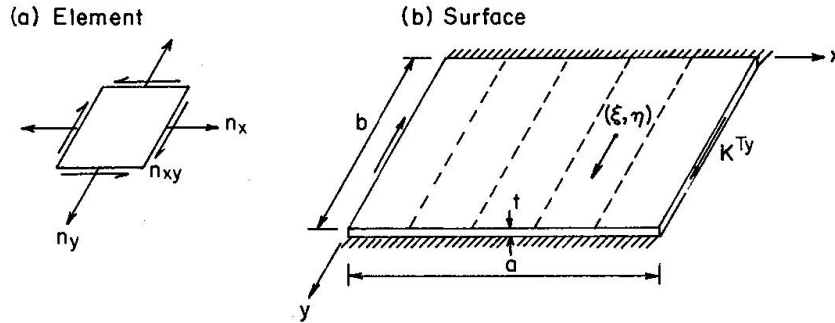(a) Element   (b) Surface

Fig. A-1. Membrane deck action.

$$u^h(x,y) = \frac{4}{a} \sum_{j=1}^{\infty} \sum_{i=0}^{\infty} \phi_i \overline{V}_{ij} \overset{*}{A}_{ij} \cos \alpha_i x \sin \overline{\alpha}_i y \tag{A-11}$$

$$\overset{*}{A}_{ij} = \frac{\overline{\alpha}_j(\overline{\alpha}_j^2 - \mu \alpha_i^2)}{(\alpha_i^2 + \overline{\alpha}_j^2)^2} \tag{A-12}$$

Many applications require use of the following more rapidly converging mixed formulas for v^h

$$v^h(x,y) = \sum_{j=1}^{\infty} \left[V_j^\$ + V_j^{a/s}\left(1 - 2\frac{x}{a}\right) + \frac{4}{a} \sum_{i=1}^{\infty} \overline{V}_{ij}\left(\overset{*}{B}_{ij} - \frac{1}{\alpha_i}\right) \sin \alpha_i x \right] \cos \overline{\alpha}_j y$$

$$0 \leq x \leq a \tag{A-13}$$

The boundary membrane shears due to known boundary displacements are:

$$n_{xy}^h \binom{0}{a}, y) = \sum_{j=1}^{\infty} [V_j^\$ \overline{T}_j^\$ \pm V_j^{a/s} \overline{T}_j^{a/s}] \cos \overline{\alpha}_j y \tag{A-14}$$

$$\begin{bmatrix} \overline{T}_j^\$ \\ \overline{T}_j^{a/s} \end{bmatrix} = -\frac{K}{2}(1 - \mu^2)\overline{\alpha}_j \left[\frac{\sinh a\overline{\alpha}_j \pm a\overline{\alpha}_j}{\cosh a\overline{\alpha}_j \pm 1} \right] \tag{A-15}$$

Series Transformation. — For a macro discrete field analysis, one typically needs to express a discrete function as a finite sinusoidal series when the function is given as a infinite sinusoidal series evaluated at evenly spaced intervals of the independent variable. Thus it is required to transform a special infinite series into a finite series; i.e.

$$f(x)\Big|_{x=\frac{a}{m}r} = \sum_{i=1}^{\infty} \overset{*}{A}_i \sin \tfrac{i\pi r}{m} = \sum_{k=1}^{m-1} A_k \sin \tfrac{k\pi r}{m} \qquad \text{(A-16a,b)}$$

The formula for the finite series coefficients, A_k, in terms of the infinite series coefficients $\overset{*}{A}_i$ (see Ref. 3) is:

$$A_k = \sum_{I=-\infty}^{+\infty} \overset{*}{A}_{2Im+k} \qquad \text{(A-17)}$$

These transformation series are often available in closed form; for example see Ref. (6).

Another typical problem is that of expressing a discrete load function, for example a set of evenly spaced concentrated loads, as a continuous function in the form of an infinite sinusoidal series. Consider the following functional form

$$\overset{*}{P}(x) = \sum_{\alpha=1}^{m-1} P(\alpha)\, \delta\left(x - \tfrac{a}{m}\alpha\right) \qquad \text{(A-18)}$$

in which the discrete load function, P, is available as a finite series, i.e.

$$P(\alpha) = \sum_{k=1}^{m-1} P_k \sin \tfrac{k\pi\alpha}{m} \qquad \text{(A-19)}$$

$$P_k = \tfrac{2}{m} \sum_{\alpha=1}^{m-1} P(\alpha) \sin \tfrac{k\pi\alpha}{m} \qquad \text{(A-20)}$$

Substituting the infinite series for the Dirac delta function in Eq. A-18 and making use of Eq. A-20 gives the following infinite series for the set of concentrated loads.

$$\overset{*}{P}(x) = \sum_{i=1}^{\infty} \tfrac{m}{b} P_i \sin \alpha_i x \qquad \text{(A-21)}$$

in which P_i is sine wise cyclic with a period of $2m$ for values of the index outside the normal finite series range of 0 thru m; i.e.,

$$P_k = P_{2Im+k} = -P_{2Im-k} = P_{k-2Im} \qquad \text{(A-22a,b,c)}$$

for all integer values of I.

Stringer Line Quantities. — In order to satisfy displacement compatability between a membrane and a set of composite stringers it is necessary to transform certain of the double infinite series in the continuous membrane analysis to mixed finite-infinite series for quantities evaluated only along stringer lines. Some of the required transformations are as follows:

$$B_{kj} = \tfrac{m}{a} \sum_{I=-\infty}^{+\infty} \overset{*}{B}_{2Im+k,\,j} \simeq \tfrac{m}{a} \overset{*}{B}_{kj}$$

$$B_{kj} = \left(\frac{a}{K}\right) \frac{1}{4m(1-\mu)\overline{D}_{kj}} \left[\frac{3-\mu}{\overline{\lambda}_j}\sinh \overline{\lambda}_j + \frac{1+\mu}{\overline{D}_{kj}}(1 - \cosh \overline{\lambda}_j \cos \tfrac{k\pi}{m})\right] \qquad \text{(A-23a,b,c)}$$

$$\bar{B}_{kj} = \frac{m}{a} \sum_{I=-\infty}^{+\infty} \overset{*}{B}_{2Im+k,\,j} \simeq \frac{m}{a} \overset{*}{B}_{kj}$$

$$\bar{B}_{kj} = \frac{\sin \frac{k\pi}{m}}{4\bar{D}_{kj}} \left[2 - \frac{(1+\mu)\,\bar{\lambda}_j \sinh \bar{\lambda}_j}{\bar{D}_{kj}} \right] \qquad\qquad\qquad \text{(A-24 a, b, c)}$$

in which $\bar{\lambda}_j = \frac{a}{m}\bar{\alpha}_j$, $\bar{D}_{kj} = \cosh \bar{\lambda}_j - \cos \frac{k\pi}{m}$ \qquad\qquad (A-25 a, b)

Stringer Analysis. — For the analysis of a deck in which the top surface is composite with the stringers, a set of beam kernel functions (often termed a Green's tensor) is required to give the longitudinal and transverse displacement fields at the top of the stringer due to independent unit impulse longitudinal and transverse loads, that is, for $N(y) = \delta(y\text{-}\eta)$ the w and v displacements are K^{wz} and K^{vz} respectively while for $F(y) = \delta(y\text{-}\eta)$ the w and v displacements are K^{wy} and K^{vy} respectively (see Fig. A-2). The required kernel functions are

$$\begin{bmatrix} K^{wz}(y,\eta) & K^{wy}(y,\eta) \\ K^{vz}(y,\eta) & K^{vy}(y,\eta) \end{bmatrix} = \frac{2}{b} \sum_{j=1}^{\infty} \begin{bmatrix} \overset{*}{A}_j \sin \bar{\alpha}_j\eta \sin \bar{\alpha}_j y & \overset{*}{D}_j \cos \bar{\alpha}_j\eta \sin \bar{\alpha}_j y \\ \overset{*}{D}_j \sin \bar{\alpha}_j\eta \cos \bar{\alpha}_j y & \overset{*}{B}_j \cos \bar{\alpha}_j\eta \cos \bar{\alpha}_j y \end{bmatrix} \quad \text{(A-26)}$$

in which

$$\overset{*}{A}_j = \frac{1}{B\bar{\alpha}_j^4}; \quad \overset{*}{D}_j = \frac{e}{B\bar{\alpha}_j^3}; \quad \overset{*}{B}_j = \frac{\rho^2 + e^2}{B\bar{\alpha}_j^2} \qquad\qquad \text{(A-27 a, b, c)}$$

B equals the flexural rigidity of the stringer, e equals the eccentricity of the longitudinal loads with respect to the stringer centroid and ρ equals the radius of gyration with respect to the cross sectional axis parallel to the deck surface. (Note that the term with $\overset{*}{B}_0$ is omitted due to the fact that $F(y)$ will be self equilibrating).
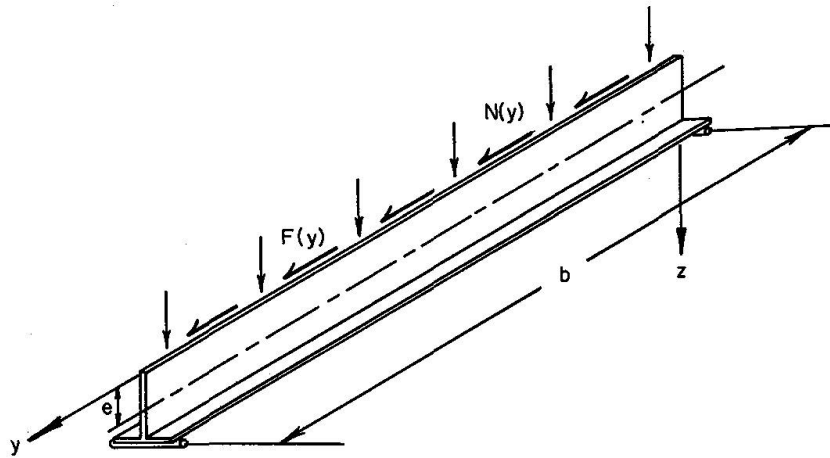

Fig. A-2. Stringer forces

In order to evaluate stringer node deflections due to a discrete loading (e.g. at the stringer-diaphragm intersections) one requires the coefficients of a discrete kernel function series A_l as follows:

$$A_l = \tfrac{n}{b} \sum_{J=-\infty}^{+\infty} \overset{*}{A}_{2Jn+l} \simeq \tfrac{n}{b} \overset{*}{A}_l \qquad \text{(A-28 a, b)}$$

$$A_l = \tfrac{1}{12B} \left(\tfrac{b}{n}\right)^3 \frac{3-\overline{\alpha}_l}{(\overline{\alpha}_l)^2}; \qquad \overline{\sigma}_l = 1 - \cos \tfrac{l\pi}{n} \qquad \text{(A-29 a, b)}$$

Notation

The following symbols are used in this paper:

$\overset{*}{A}_i$, $\overset{*}{A}_k$	coefficients of infinite and finite series.
$\overset{*}{A}_j$, $\overset{*}{B}_j$, $\overset{*}{D}_j$	coefficients of stringer kernel functions.
$\overset{*}{A}_{ij}$, $\overset{*}{B}_{ij}$ A_{ij}, B_{ij}	coefficients of infinite kernel function series.
a, b	plate dimensions.
B	flexural rigidity of stringer.
B_{kj}, $\overline{B}_{kj}$	coefficients of discrete kernel function series.
$\underline{D}_x$, D_y	differential operators.
$\overline{D}_{kj}$	series parameter (Eq. A-25).
E	Youngs modulus.
e	eccentricity of membrane forces.
$H(r,y)$, H_{kj}	membrane — stringer interactive force and series coefficients.
i, j	indices for infinite series.
K	membrane plate stiffness.
K^{uy}, K^{vy}, K^{Ty}	membrane kernel functions.
k, l	indices for finite series.
m, n	limits of finite series indices.
$N(r,y)$ N_{kj}	applied stringer load and series coefficients.
$\underset{*}{N}_x$, N_{xy}, N_y	membrane stress resultants.
$\overset{*}{P}(x)$, $P(\alpha)$	continuous and discrete load functions.
$P_j^\$$, $P_j^{a/s}$	coefficients of boundary stringer load series.
$\underline{R}(r,s)$, R_{kl}	stringer-diaphragm interactive forces and series coefficients.
$\overline{T}_j^\$$, $T_j^{a/s}$	coefficients of boundary shear.
t	plate thickness.
u, v	membrane displacements.
$V_j^\$$, $V_j^{a/s}$, $\overline{V}_{ij}$	coefficients of boundary displacements.
$w(r,y)$	out-of-plane stringer displacements.
x, y	continuous coordinates.
α_i, $\overline{\alpha}_j$	$\tfrac{i\pi}{a}$, $\tfrac{j\pi}{b}$ respectively.
δ_j^o, $\delta(x-\eta)$	Kronecker and Dirac delta functions.
$\overline{\lambda}_j$	series parameter (Eq. A-25).

μ Poisson's ratio.
ξ, η impulse load coordinates.
ρ_* radius of gyration of stringer.
ϕ_j weighting function.

Practical implications

The thin element or metal plate-stringer-diaphragm bridge deck in either cellular or orthotropic form is one of the most efficient load carrying systems employed by designers today and the literature includes many references to recommended methods of analysis. However, none of the existing methods are rationally based even though some are rather complex and require voluminous computations.

New formulas are presented herein for the exact elastic analysis of plate-stringer-diaphragm bridge deck systems that 1) are proportioned and detailed so that all components have negligible out-of-plane stiffness and 2) are simply supported at the ends. The formulas are unrestricted as to range of parameters in the structural class; that is, they apply equally well to decks with small edge beams with diaphragms serving as transverse load distributers and to decks with primary support by the edge girders with diaphragms serving as floor beams. Minor modification of the formulas permits their use for symmetrical sandwich decks and for decks continuous over intermediate supports.

It is proposed that these exact formulas be used for final design review. They are in the form of double sinusoidal series and can be programmed for use of desk top or miniature computers or simplified for manual calculations through truncation of the series. The formulas can also serve as a standard analysis for use in studying existing and proposed approximate formulas in order to establish range of applicability, magnitude of errors, etc. This should obviate the unsatisfactory practice of making judgements based upon comparison of one empirical method with another empirical method.

Existing alternatives to the proposed method are: 1) use of code sanctioned empirical formulas to compute an "effective flange width" for the stringers and to compute distribution of loads between the resulting "T" beams; 2) use of a "smearing out" technique to replace the mixed discrete-continuous system by an "equivalent" (usually orthotropic) continuum and 3) use of a discrete or latticed system to approximate the real system through a finite difference or finite element approach. The "equivalent continuum" method lacks rational bases for selecting the substitute continuum and for applying the results to the real system. The errors introduced are significant for coarse lattices and for decks with stiff ribs. The finite element version of the substitute lattice approach is superior to the substitute continuum approach but lacks well-developed error analyses. Also, its use for numerous alternate designs is quite expensive due to the voluminous computations and the extensive input data required for each case. For example, the relatively coarse finite element network used to check one of the numerical examples required two orders of magnitude more computing time than did the formula approach and nearly three orders of magnitude more input information.

It is hoped that this introduction of a rational analysis for orthotropic bridge decks will encourage expanded use by designers of this attractive system, especially in those countries where they are not presently in popular use.

References

1. CHEUNG, Y.K., KING, I.P., and ZIENKIEWICZ, O.C.: Slab Bridges With Arbitrary Shape and Support Conditions: A General Method of Analysis Based on Finite Elements. The Institute of Civil Engineering, London, Vol. 40, May 1968, pp. 9–36.
2. DEAN, D.L., and OMID'VARAN, C.: Analysis of Ribbed Plates. Journal of the Structural Division, ASCE, Vol. 95, No. ST3, March 1969, pp. 411–440.
3. DEAN, D.L., and GANGARAO: Macro Approach to Discrete Field Analysis, Journal of the Engineering Mechanics Division, ASCE, Vol. 96, No. EM4, August 1970, pp. 377–394.
4. DEAN, D.L., and ABDEL-MALEK, R.A.: Rational Analysis of Orthotropic Bridge Decks. International Journal of Mechanical Sciences, Pergamon Press, Vol. 16, 1974, pp. 173–192.
5. Design Manual for Orthotropic Steel Plate Deck Bridges: AISC, New York, 1961.
6. JOLLEY, L.B.W.: Summation of Series. Dover Publications, Inc., New York, 1961.
7. POWELL, G.H., and OGDEN, D.W.: Analysis of Orthotropic Steel Plate Bridge Decks. Journal of the Structural Division, ASCE, Vol. 95, No. ST5, May 1969, pp. 909–922.
8. Standard Specifications for Highway Bridges: The American Association of State Highway Officials, 10th Edition, 1969, Washington, D.C., pp. 28–31.
9. TRIOTSKY, M.S.: Orthotropic Bridges Theory and Design. James, F. Lincoln Arc Welding Foundation, Cleveland, Ohio, August 1967, pp. 53–213.

Summary

Formulas are introduced which provide the designer with an exact elastic analysis of thin element bridge decks consisting of a set of evenly spaced stringers that are composite with a rectangular plate and are braced by a set of evenly spaced diaphragms. The system is simply supported at the ends with simple or flexible side supports. The loading consists of an arbitrary distribution of stringer line loads. The solution is readily modified to analyze cellular decks or, through superposition, decks with intermediate supports.

Résumé

On introduit des formules fournissant au projeteur une analyse élastique exacte d'éléments minces de tabliers composés d'un groupe de poutres longitudinales réparties à distances égales et jointes avec une plaque rectangulaire et renforcées par des diaphragmes répartis à distances égales. Le système est simplement supporté aux extrémités par des supports latéraux simples ou flexibles. La charge agit par une distribution arbitraire de charges linéaires. La solution est légèrement modifiée pour l'analyse des tabliers cellulaires ou, par superposition de tabliers avec supports intermédiaires.

Zusammenfassung

Es werden Formeln eingeführt, die dem Projektbearbeiter eine genaue elastische Analyse dünner Fahrbahnelemente liefern, welche aus einem Satz in gleichem Abstand verteilter Längsträger bestehen, die mit einer Rechteckplatte verbunden und durch eine Anzahl in gleichem Abstand verteilter Diaphragmen versteift sind. Das System wird an den Enden durch einfache oder flexible seitliche Auflager gestützt. Die Belastung besteht aus einer beliebig verteilten Längsträger-Linienlast. Die Lösung lässt sich leicht modifizieren, je nachdem es sich um zellenförmige Fahrbahnen oder, durch Übereinanderlagern, um Fahrbahnen mit zwischenliegenden Auflagern handelt.